

First Experimental Constraints on WIMP Couplings in Effective Field Theory Framework from the CDEX Experiment

Y. Wang,^{1,2} Z. Zeng,¹ Q. Yue,^{1,*} L. T. Yang,^{1,†} K. J. Kang,¹ Y. J. Li,¹ M. Agartioglu,^{3,4,‡} H. P. An,^{1,2} J. P. Chang,⁵ J. H. Chen,^{3,‡} Y. H. Chen,⁶ J. P. Cheng,^{1,7} C. Y. Chiang,^{3,‡} W. H. Dai,¹ Z. Deng,¹ X. P. Geng,¹ H. Gong,¹ Q. J. Guo,⁸ X. Y. Guo,⁶ L. He,⁵ S. M. He,⁶ J. W. Hu,¹ T. S. Huang,⁹ H. X. Huang,¹⁰ H. T. Jia,¹¹ L. P. Jia,¹ H. B. Li,^{3,‡} J. M. Li,¹ J. Li,¹ M. X. Li,¹¹ R. M. J. Li,¹¹ X. Li,¹⁰ Y. L. Li,¹ B. Liao,⁷ F. K. Lin,^{3,‡} S. T. Lin,¹¹ S. K. Liu,¹¹ Y. D. Liu,⁷ Y. Y. Liu,⁷ Z. Z. Liu,¹ H. Ma,¹ Y. C. Mao,⁸ Q. Y. Nie,¹ J. H. Ning,⁶ H. Pan,⁵ N. C. Qi,⁶ C. K. Qiao,¹¹ J. Ren,¹⁰ X. C. Ruan,¹⁰ C. S. Shang,⁶ V. Sharma,^{3,12,‡} Z. She,¹ L. Singh,^{3,12,‡} M. K. Singh,^{3,12,‡} T. X. Sun,⁷ C. J. Tang,¹¹ W. Y. Tang,¹ Y. Tian,¹ G. F. Wang,⁷ L. Wang,¹³ Q. Wang,^{1,2} Y. X. Wang,⁸ Z. Wang,¹¹ H. T. Wong,^{3,‡} S. Y. Wu,⁶ Y. C. Wu,¹ H. Y. Xing,¹¹ Y. Xu,¹⁴ T. Xue,¹ Y. L. Yan,¹¹ N. Yi,¹ C. X. Yu,¹⁴ H. J. Yu,⁵ J. F. Yue,⁶ M. Zeng,¹ B. T. Zhang,¹ L. Zhang,¹¹ F. S. Zhang,⁷ M. G. Zhao,¹⁴ J. F. Zhou,⁶ Z. Y. Zhou,¹⁰ and J. J. Zhu¹¹

(CDEX Collaboration)

¹Key Laboratory of Particle and Radiation Imaging (Ministry of Education) and Department of Engineering Physics, Tsinghua University, Beijing 100084

²Department of Physics, Tsinghua University, Beijing 100084

³Institute of Physics, Academia Sinica, Taipei 11529

⁴Department of Physics, National Dong Hwa University, Hualien 97401

⁵NUCTECH Company, Beijing 100084

⁶YaLong River Hydropower Development Company, Chengdu 610051

⁷College of Nuclear Science and Technology, Beijing Normal University, Beijing 100875

⁸School of Physics, Peking University, Beijing 100871

⁹Sino-French Institute of Nuclear and Technology, Sun Yet-sen University, Zhuhai 519082

¹⁰Department of Nuclear Physics, China Institute of Atomic Energy, Beijing 102413

¹¹College of Physics, Sichuan University, Chengdu 610065

¹²Department of Physics, Banaras Hindu University, Varanasi 221005

¹³Department of Physics, Beijing Normal University, Beijing 100875

¹⁴School of Physics, Nankai University, Tianjin 300071

(Dated: July 31, 2020)

We present weakly interacting massive particles (WIMPs) search results with two approaches of effective field theory from the China Dark Matter Experiment (CDEX), based on the data from both CDEX-1B and CDEX-10 stages. In the non-relativistic effective field theory approach, both time-integrated and annual modulation analysis have been used to set new limits on the coupling of WIMP-nucleon effective operators at 90% confidence level (C.L.) and improve over the current bounds in the low m_χ region. In the chiral effective field theory approach, data from CDEX-10 are used to set an upper limit on WIMP-pion coupling at 90% C.L. We have extended the limit to the $m_\chi < 6$ GeV/ c^2 region for the first time.

PACS numbers: 95.35.+d, 29.40.-n, 98.70.Vc

Introduction. Throughout the past decades, compelling evidences from astroparticle physics and cosmology indicate the existence of dark matter (DM) [1]. The leading candidate for cold dark matter, weakly interacting massive particles (WIMPs, denoted as χ) have been actively searched via spin-independent (SI) and spin-dependent (SD) elastic scattering with normal matter in underground direct detection experiments [2–12]. However, the standard SI and SD scattering calculations are derived from the leading-order terms in WIMP-nucleon effective field theory (EFT) with ordinary treatment of nuclear structure [13–15]. In order to explore different possible WIMP-nucleus interactions, two alternative schemes of EFT, non-relativistic effective field theory (NREFT) [16–19] and chiral effective field theory (ChEFT) [20–22], have been proposed and the conse-

quences have been examined by several direct detection experiments [23–27].

The China Dark Matter Experiment (CDEX) [8, 28–36], aiming at direct detection of light DM with p -type point contact germanium (PPCGe) detectors, has finished two phases of data taking—namely CDEX-1(A, B) and CDEX-10. An energy threshold of 160 eV was achieved in CDEX-1B [33] and CDEX-10 [8], which enhances sensitivities for light DM. In this letter, we report the results of EFT analysis based on the data from CDEX-1B [33, 34] and CDEX-10 [8, 36]. In addition, the long-duration data and stable running conditions of CDEX-1B[34] allows annual modulation (AM) analysis to be performed as a new aspect of EFT studies.

EFT approaches. In NREFT approach, all leading-order and next-to-leading order operators maintaining

Galilean-invariance are taken into consideration [16–19]. This approach introduces 14 operators, \mathcal{O}_i ($i = 1, 3-15$) [19], which rely on different types of nuclear responses in addition to the standard SI and SD cases. These operators depend explicitly on WIMP and nucleon spins, \vec{S}_χ and \vec{S}_N , the relative perpendicular velocity between the WIMP and the nucleon, \vec{v}^\perp , in addition to the momentum transfer \vec{q} . Note that \mathcal{O}_2 is not considered here since it cannot be obtained from a relativistic operator at leading order [18, 19].

The differential scattering rate with respect to nuclear recoil energy in direct detection is generally given by:

$$\frac{dR}{dE_R} = \frac{\rho}{m_\chi m_A} \int_{v_{\min}(E_R)} v f(\mathbf{v}) \frac{d\sigma}{dE_R} d^3v \quad (1)$$

where $\rho = 0.3 \text{ GeV}/(c^2 \text{ cm}^3)$ is the local DM density, m_χ and m_A are the masses of the WIMP and target nucleus respectively, v is the relative velocity of WIMP in the lab-frame, v_{\min} is the minimal WIMP velocity that could induce a nuclear recoil for a given energy E_R and $f(v)$ is a Maxwellian velocity distribution with a most probable speed of $v_0 = 220 \text{ km/s}$ and a galactic escape velocity of $v_{\text{esc}} = 544 \text{ km/s}$.

As discussed in Ref. [19], the details of particle physics arising from NREFT are contained in the differential cross section $d\sigma/dE_R$, associated with those 14 space-spin operators which are coupled to protons and neutrons distinctly. Considering the isoscalar case, where the operators (\mathcal{O}_i) are coupled to protons and neutrons equally, the strength of NREFT interaction is parameterized by coefficients c_i^0 (0 denotes the “isoscalar” case) which have dimensions of $1/\text{energy}^2$, such that they are multiplied by weak mass scale ($m_W = 246.2 \text{ GeV}/c^2$) to be dimensionless. The results of NREFT framework presented in this letter are based on pure-isoscalar couplings. The expected recoil energy spectra of each WIMP mass for each EFT operator are calculated by a *Mathematica* script introduced in Ref. [18, 19]. The spectra of \mathcal{O}_1 , \mathcal{O}_5 , \mathcal{O}_6 and \mathcal{O}_{15} are displayed in Fig. 1(a). The different dependence on momentum transfer of these operators gives rise to different suppression of event rates at low energies in the corresponding spectra.

As is well known, the Earth’s velocity relative to the galactic WIMP halo is time varying with a period of one year, and can be expressed as $v_E(t) = \{232 + 30 \times 0.51 \cos 2\pi(t - \phi)/T\} \text{ km/s}$, where T is 365.25 days, ϕ is 152.5 days from January 1st. Positive observations of AM would provide smoking-gun signatures for WIMP-nuclei scattering rates, as shown in Fig. 1(b), and the modulation amplitudes are proportional to isoscalar coefficients $(c_i^0)^2$. As discussed in Ref. [19], these operators are classified as leading order, next-to-leading order and next-to-next-to-leading order, depending on the total number of momenta and velocities involved. The cross sections of

different operators are scaled by $(v^2)^\alpha$, where α is the total number of momenta and velocities in these operators. Compared with \mathcal{O}_1 , where the cross section is scaled by v^0 , the modulation amplitude of \mathcal{O}_8 is larger since its cross section is scaled by v^2 .

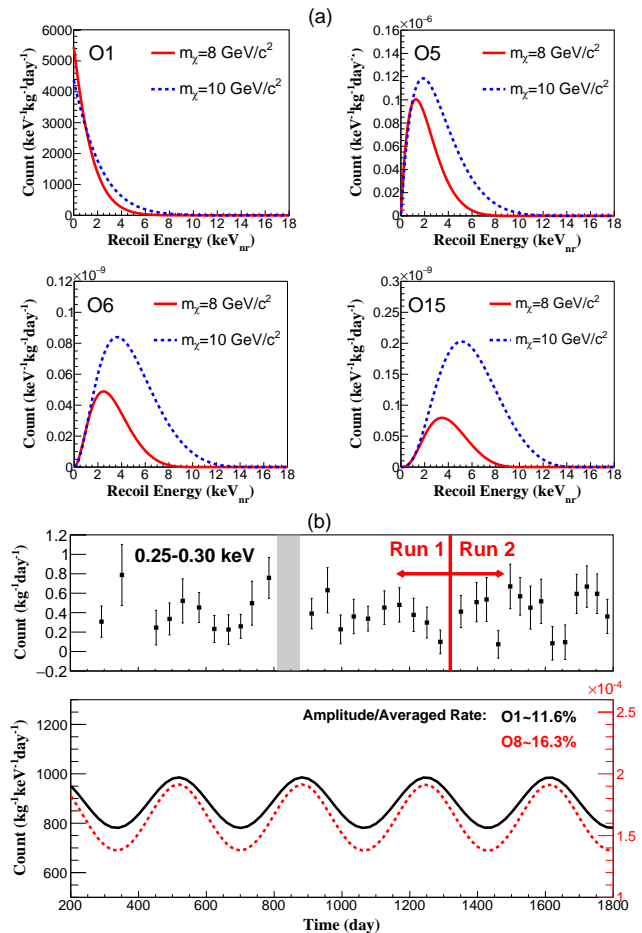


FIG. 1. (a) Expected recoil spectra of isoscalar operator \mathcal{O}_1 , \mathcal{O}_5 , \mathcal{O}_6 and \mathcal{O}_{15} for elastic scattering of $8 \text{ GeV}/c^2$ and $10 \text{ GeV}/c^2$ WIMPs on germanium nuclei, with $c_i^0 = 1$. The event rates of $\mathcal{O}_{5,6,15}$ are suppressed at low energies as they depend on the momentum transfer in form of $\sim q^2$, q^4 and q^6 respectively. (b) The top graph shows bulk event count versus time in energy bin of $0.25\text{--}0.30 \text{ keV}$ and the shaded area denotes the period of gamma source calibration. The details of these data are explained in Ref. [34]. The bottom graph displays the modulated event rates of \mathcal{O}_1 and \mathcal{O}_8 in the same energy bin of $0.25\text{--}0.30 \text{ keV}$. The mass of WIMPs was set to be $5 \text{ GeV}/c^2$, and $c_{1,8}^0 = 1$.

The ChEFT approach predicts consistent couplings of WIMPs to two nucleons by pion-exchange [20–22]. This letter focuses on ChFET in the SI channel, in which the leading two-body currents [37–44] cannot be absorbed into a redefinition of the WIMP-nucleon coupling. The new couplings (denoted as $\sigma_{\chi\pi}^{\text{scalar}}$) are interpreted as cross sections for a WIMP scattering off a pion exchanged between two nucleons [44, 45]. The inclusion of the leading

two-body currents in SD channel is a correction to the standard response and is expected to have a significant impact on SD searches [46–50]. However, this study is beyond the scope of the current work.

The two-body currents of the SI channel in ChEFT framework involve a new combination of hadronic matrix elements and Wilson coefficients c_π , and constitute the most important coherent corrections [51]. Therefore, in the scenario without standard SI interactions, the WIMP-nucleon (χ - \mathcal{N}) cross section are expressed in terms of the scalar WIMP-pion cross section $\sigma_{\chi\pi}^{\text{scalar}}$ and WIMP-pion reduced mass μ_π : $d\sigma_{\chi\mathcal{N}}^{\text{SI}}/dq^2 = d\sigma_{\chi\pi}^{\text{scalar}}/\mu_\pi^2 v^2 |\mathcal{F}_\pi(q^2)|^2$, $d\sigma_{\chi\mathcal{N}}^{\text{scalar}} = \mu_\pi^2/4\pi |c_\pi|^2$, where q is momentum transfer and \mathcal{F}_π is the nuclear structure factor. The calculation of structure factor \mathcal{F}_π has been discussed in details in Ref. [44]. For a given WIMP mass m_χ , the differential event rate for the WIMP-pion coupling can be written as

$$\frac{dR}{dE_R} = \frac{2\rho\sigma_{\chi\pi}^{\text{scalar}}}{m_\chi\mu_\pi^2} \times |\mathcal{F}_\pi(q^2)|^2 \times \int_{v_{\min}(E_R)} f(\mathbf{v}) d^3v. \quad (2)$$

The spectra of WIMP-pion scattering are displayed in Fig. 2(a). Based on Eq. (2), we can derive the limits for $\sigma_{\chi\pi}^{\text{scalar}}$ as a function of the WIMP mass m_χ . Estimated from the nuclear structure factors, the coupling to pion is subleading compared with SI, but dominant over SD scattering [45], therefore making it be highly valued in the analyses of WIMPs.

Results of NREFT. Both time integrated (TI) analysis and AM analysis are applied in the current analysis, using the data from CDEX-1B and CDEX-10.

In TI analysis, the final constraints on the operators \mathcal{O}_i are calculated independently, based on two different datasets from CDEX-1B and CDEX-10 with exposures of 737.1 kg-day and 205.4 kg-day, respectively. The data used in this analysis have been selected after a series of criteria [8, 33] and the data of CDEX-10 are only from the detector with best performance, named C10-B1 [36].

For CDEX-10 data, the minimum- χ^2 analysis [30] and unified approach [52] are applied to the residual spectrum, from which the contributions of L/M -shell x-ray peaks have been subtracted by fitting corresponding K -shell x-ray peaks, as shown in Fig. 2(b). However, for CDEX-1B, the background of unknown origin at low energy region below 2 keV makes minimum- χ^2 analysis inapplicable and a Binned Poisson method is used as substitute [53]. For both CDEX-10 and CDEX-1B, a 10% systematic error is adopted for the quenching factor calculated by TRIM package [54–57]. The upper limits at 90% confidence level (C.L.) on 14 different operators based on CDEX-1B and CDEX-10 are shown Fig. 3, in which the results of SuperCDMS [23], XENON100 [24] and CRESST-II [25] are superimposed as comparison. We note that PandaX-II [26] and LUX [27] have also released results on EFT studies, but with relativistic EFT

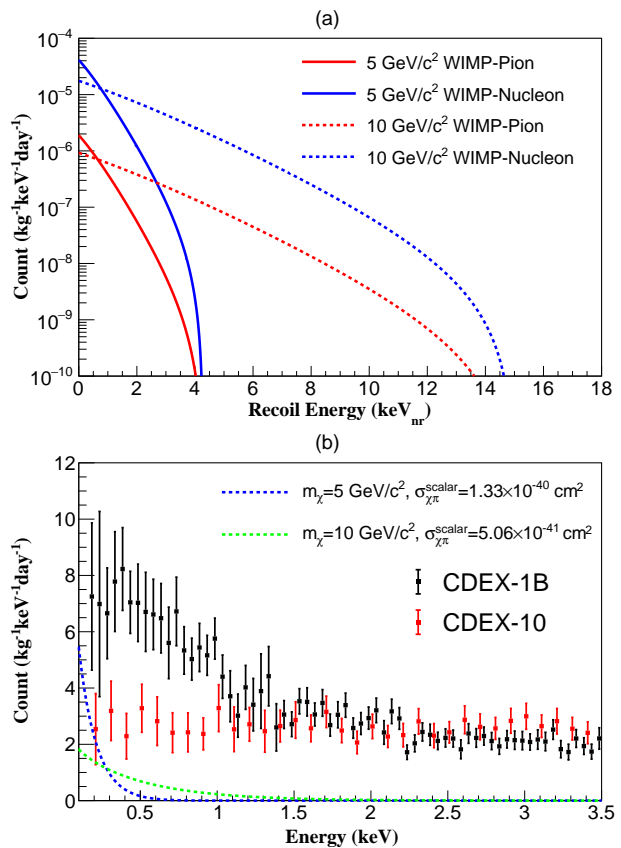


FIG. 2. (a) Differential recoil spectrum for WIMP-pion (red) and SI WIMP-nucleon (blue) interactions at masses of 5 GeV/ c^2 and 10 GeV/ c^2 respectively, with cross sections of 1×10^{-46} cm 2 . (b) The residual spectra of C10-B1 (red points) and CDEX-1B (black points). The blue dotted line and green dotted line are the expected χ - \mathcal{N} spectra due to WIMP-pion scattering at m_χ equal to 5 GeV/ c^2 and 10 GeV/ c^2 respectively, at cross section corresponding to the upper limits at 90% C.L., derived from CDEX-10 dataset.

or pure-proton/neutron framework. Direct comparisons of both results would be infeasible. It can be seen that CDEX-10 data provide more stringent constraints over the current bounds in the m_χ range from 2.5 up to several GeV/ c^2 in all the operators studied as a consequence of the low physics analysis threshold.

In AM analysis, data from CDEX-1B at 0.25–5.80 keV are analyzed following the same procedure in Ref [34]. The total exposure is 1107.5 kg-day within a total time span 1527 calendar days (~ 4.2 yr), including two runs (Run-1 and Run-2). Using the same AM analysis procedures of our previous work[34, 35], we present the 90% C.L. upper limits of $(c_i^0)^2$ in Fig. 3, together with the results of TI analysis. The operators with higher order of velocity dependence (all except $\mathcal{O}_{1,4}$) give larger annual modulation amplitudes. Accordingly as indicated in Fig. 3, with the similar CDEX-1B data set, the AM analysis for these operators could give more stringent

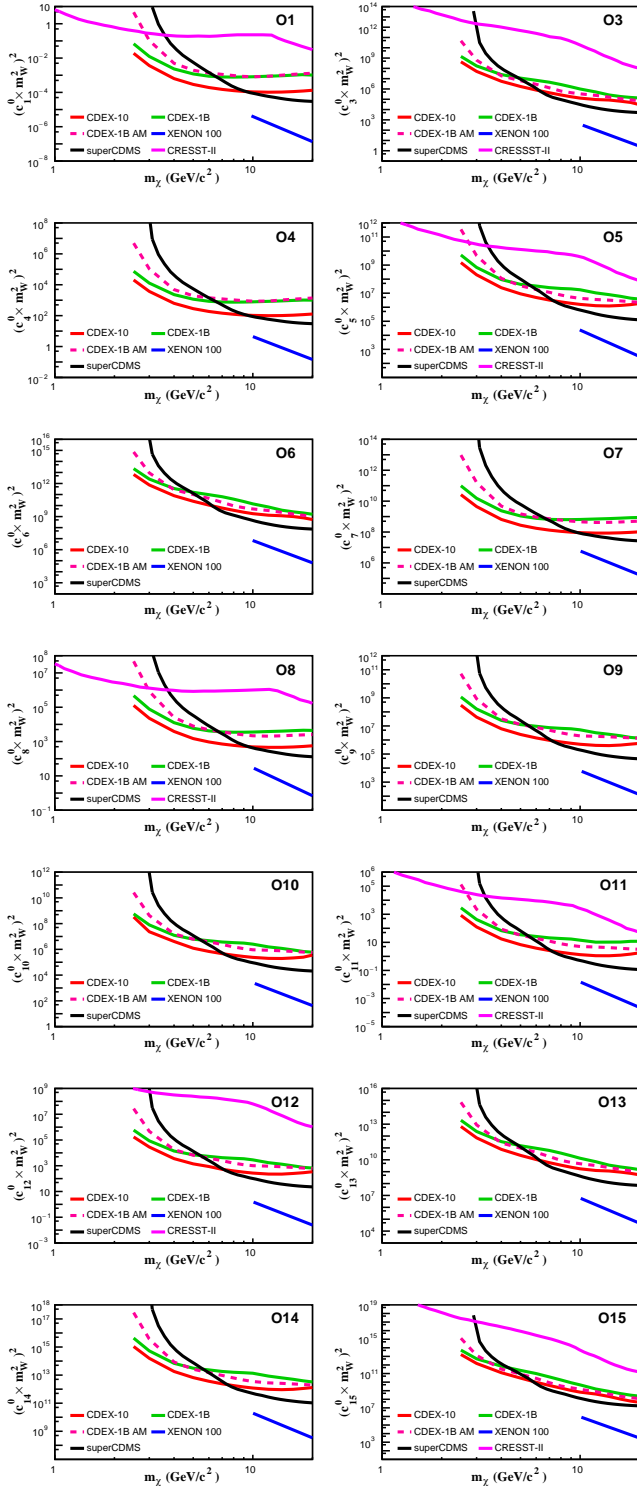


FIG. 3. The 90% C.L. upper limits of CDEX-10 and CDEX-1B on isoscalar dimensionless coupling for all NREFT operators. The TI results of CDEX-10 and CDEX-1B are indicated in solid red and green respectively, while the AM results of CDEX-1B are presented as pink dashes. The limits from superCDMS [23], XENON100 [24] and CRESST-II [25] are indicated in solid black, blue, and magenta respectively.

constraints on coupling coefficients than the TI analysis in m_χ region above several GeV/c^2 . This behavior is different from the standard AM/TI analysis on the SI channel [34], in which the constraints with TI are more stringent than those of AM over the entire range of m_χ .

Result of WIMP-pion scattering in ChEFT. For WIMP-pion scattering in ChEFT framework, the minimum- χ^2 analysis, analogous to that used in TI analysis for NREFT, is applied to the data of CDEX-10 with an exposure of 205.4 kg-day. The exclusion plot of scalar WIMP-pion coupling at 90% C.L. is depicted in Fig. 4, superimposed with the results given by XENON1T [45]. The low energy threshold of CDEX-10 brings along improved sensitivities for low-mass WIMPs and gives rise to new constraints on WIMP-pion cross section at $m_\chi < 6 \text{ GeV}/c^2$.

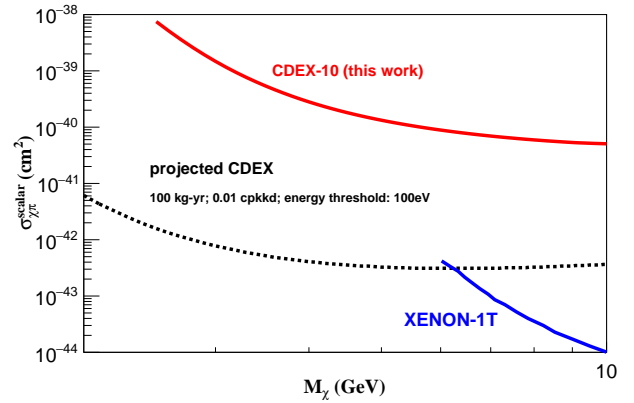


FIG. 4. Upper limit at 90% C.L. on the WIMP-pion coupling as a function of WIMP mass for CDEX-10 (red), superimposed with the results (blue) given by XENON1T experiment [45]. The potential reach with target sensitivities of 100 eV threshold at 0.01 counts $\text{kg}^{-1}\text{keV}^{-1}\text{day}^{-1}$ (cpkdd) background level for 100 kg-year exposure are also displayed here.

Summary. Since the allowed regions of the standard SI and SD are further probed and excluded by the various direct detection experiments [9–12], the analyses of new channels, such as NREFT operators and WIMP-pion coupling from ChEFT, are motivating new directions to DM direct detection experiments. With incorporating the NREFT to the analysis of the CDEX data, the upper limits on isoscalar coupling are set by both TI and AM analysis at 2.5–20 GeV/c^2 of m_χ and new parameters spaces are excluded at 90% C.L. As for WIMP-pion coupling, CDEX-10 gives new constraints on WIMP-pion cross section at $m_\chi < 6 \text{ GeV}/c^2$. By improving the performance of the detectors and suppressing the background, CDEX-10 is expected to give more stringent constraints on WIMP couplings in the EFT framework.

This work was supported by the National Key Research and Development Program of China (Grant No. 2017YFA0402200) and the National Natural Sci-

ence Foundation of China (Grants No. 11725522, No. 11675088, No. 11475099, No. U1865205). We are grateful to Y.F. Zhou for helpful discussion.

* Corresponding author: yueq@mail.tsinghua.edu.cn

† Corresponding author: yanglt@mail.tsinghua.edu.cn

‡ Participating as a member of TEXONO Collaboration

- [1] M. Tanabashi *et al.* (Particle Data Group), Phys. Rev. D **98**, 030001 (2018).
- [2] E. Armengaud *et al.* (EDELWEISS Collaboration), J. Cosmol. Astropart. Phys. **05**, 019 (2016).
- [3] D. S. Akerib *et al.* (LUX Collaboration), Phys. Rev. Lett. **118**, 021303 (2017).
- [4] C. Amole *et al.* (PICO Collaboration), Phys. Rev. Lett. **118**, 251301 (2017).
- [5] X. Cui *et al.* (PandaX-II Collaboration), Phys. Rev. Lett. **119**, 181302 (2017).
- [6] P. A. Amaudruz *et al.* (DEAP-3600 Collaboration), Phys. Rev. Lett. **121**, 071801 (2018).
- [7] K. Abe *et al.* (XMASS Collaboration), Phys. Lett. B **789**, 45 (2019).
- [8] H. Jiang *et al.* (CDEX Collaboration), Phys. Rev. Lett. **120**, 241301 (2018).
- [9] G. Angloher *et al.* (CRESST Collaboration), The Eur. Phys. J. C **76**, 25 (2016).
- [10] R. Agnese *et al.* (SuperCDMS Collaboration), Phys. Rev. Lett. **120**, 061802 (2018).
- [11] P. Agnes *et al.* (DarkSide Collaboration), Phys. Rev. Lett. **121**, 081307 (2018).
- [12] E. Aprile *et al.* (XENON Collaboration), Phys. Rev. Lett. **123**, 251801 (2019).
- [13] J. Lewin and P. Smith, Astropart. Phys. **6**, 87 (1996).
- [14] M. T. Ressell, M. B. Aufderheide, S. D. Bloom, K. Griest, G. J. Mathews, and D. A. Resler, Phys. Rev. D **48**, 5519 (1993).
- [15] V. I. Dimitrov, J. Engel, and S. Pittel, Phys. Rev. D **51**, R291 (1995).
- [16] J. Fan, M. Reece, and L. T. Wang, J. Cosmol. Astropart. Phys. **11**, 042 (2010).
- [17] B. A. Dobrescu and I. Mocioiu, J. High Energy Phys. **11**, 005 (2006).
- [18] A. L. Fitzpatrick, W. Haxton, E. Katz, N. Lubbers, and Y. Xu, J. Cosmol. Astropart. Phys. **2013**, 004 (2013).
- [19] N. Anand, A. L. Fitzpatrick, and W. C. Haxton, Phys. Rev. C **89**, 065501 (2014).
- [20] E. Epelbaum, H.-W. Hammer, and U.-G. Meißner, Rev. Mod. Phys. **81**, 1773 (2009).
- [21] R. Machleidt and D. Entem, Phys. Rep. **503**, 1 (2011).
- [22] H.-W. Hammer, A. Nogga, and A. Schwenk, Rev. Mod. Phys. **85**, 197 (2013).
- [23] K. Schneck *et al.* (SuperCDMS Collaboration), Phys. Rev. D **91**, 092004 (2015).
- [24] E. Aprile *et al.* (XENON Collaboration), Phys. Rev. D **96**, 042004 (2017).
- [25] G. Angloher *et al.* (CRESST Collaboration), Eur. Phys. J. C **79**, 021303 (2019).
- [26] J. Xia *et al.* (PandaX-II Collaboration), Phys. Lett. B **792**, 193 (2019).
- [27] D. S. Akerib *et al.* (LUX Collaboration), (2020), arXiv:2003.11141 [astro-ph.CO].
- [28] K. J. Kang *et al.*, Front. Phys. **8**, 412 (2013).
- [29] W. Zhao *et al.* (CDEX Collaboration), Phys. Rev. D **88**, 052004 (2013).
- [30] Q. Yue *et al.* (CDEX Collaboration), Phys. Rev. D **90**, 091701 (2014).
- [31] W. Zhao *et al.* (CDEX Collaboration), Phys. Rev. D **93**, 092003 (2016).
- [32] L. Wang *et al.* (CDEX Collaboration), Sci. China-Phys. Mech. Astron **60**, 071011 (2017).
- [33] L. T. Yang *et al.* (CDEX Collaboration), Chin. Phys. C **42**, 023002 (2018).
- [34] L. T. Yang *et al.* (CDEX Collaboration), Phys. Rev. Lett. **123**, 221301 (2019).
- [35] Z. Z. Liu *et al.* (CDEX Collaboration), Phys. Rev. Lett. **123**, 161301 (2019).
- [36] Z. She *et al.* (CDEX Collaboration), Phys. Rev. Lett. **124**, 111301 (2020).
- [37] V. Cirigliano, M. L. Graesser, and G. Ovanessian, J. High Energy Phys. **10**, 025 (2012).
- [38] V. Cirigliano, M. L. Graesser, G. Ovanessian, and I. M. Shoemaker, Phys. Lett. B **739**, 293 (2014).
- [39] M. Hoferichter, P. Klos, and P. Schwenk, Phys. Lett. B **746**, 410 (2015).
- [40] M. Hoferichter, P. Klos, J. Menéndez, and A. Schwenk, Phys. Rev. D **94**, 063505 (2016).
- [41] C. Körber, A. Nogga, and J. de Vries, Phys. Rev. C **96**, 035805 (2017).
- [42] M. Hoferichter, P. Klos, J. Menéndez, and A. Schwenk, Phys. Rev. Lett. **119**, 181803 (2017).
- [43] L. Andreoli, V. Cirigliano, S. Gandolfi, and F. Pederiva, Phys. Rev. C **99**, 025501 (2019).
- [44] M. Hoferichter, P. Klos, J. Menéndez, and A. Schwenk, Phys. Rev. D **99**, 055031 (2019).
- [45] E. Aprile *et al.* (XENON Collaboration), Phys. Rev. Lett. **122**, 071301 (2019).
- [46] E. Aprile *et al.* (XENON100 Collaboration), Phys. Rev. Lett. **111**, 021301 (2013).
- [47] H. Uchida *et al.* (XMASS-I Collaboration), Prog. Theor. Exp. Phys. **2014**, 063C01 (2014).
- [48] E. Aprile *et al.* (XENON Collaboration), Phys. Rev. D **94**, 122001 (2016).
- [49] C. Fu *et al.* (PandaX-II Collaboration), Phys. Rev. Lett. **120**, 049902 (2018).
- [50] D. S. Akerib *et al.* (LUX Collaboration), Phys. Rev. Lett. **118**, 251302 (2017).
- [51] J. Goodman, M. Ibe, A. Rajaraman, W. Shepherd, T. M. P. Tait, and H. Yu, Phys. Rev. D **82**, 116010 (2010).
- [52] G. J. Feldman and R. D. Cousins, Phys. Rev. D **57**, 3873 (1998).
- [53] C. Savage, K. Freese, P. Gondolo, and D. Spolyar, J. Cosmol. Astropart. Phys. **04**, 010 (2009).
- [54] A. Soma *et al.*, Nucl. Instrum. Methods Phys. Res., Sect. A **836**, 67 (2016).
- [55] J. F. Ziegler, Nucl. Instrum. Methods Phys. Res., Sect. B **219-220**, 1027 (2004).
- [56] S. T. Lin *et al.* (TEXONO Collaboration), Phys. Rev. D **79**, 061101 (2009).
- [57] B. J. Scholz, A. E. Chavarria, J. I. Collar, P. Privitera, and A. E. Robinson, Phys. Rev. D **94**, 122003 (2016).